RESEARCH   **Open Access**

The role of brain structural magnetic resonance imaging in the assessment of hippocampal subfields in Alzheimer's disease

Sameh Hany Sobhy Saad[1], Mohammad Mahmoud Alhousini Alashwah[2*], Ashraf Abo Alsafa[3] and Mahmoud A. Dawoud[2]

Abstract

Background: Volumetric MR neuroimaging can visualize the pattern of hippocampal subfield atrophic changes in AD. This can be used as a biomarker in early diagnosis of AD and allow early treatment to improve memory, behavioral symptoms, and delay the cognitive deterioration. The aim of this work is to assess the role of the volumetric study of different hippocampal subfields as a post-processing technique of structural MR imaging in patients with Alzheimer's disease of different severity of cognitive functions. The regional ethics committee approved the study and written informed consent was obtained from all participants. In the duration from 2016 to 2018, a cross-sectional study was conducted on 30 patients (17 males and 13 females) and 15 healthy elderly controls (9 males and 6 females) referred to the Radiodiagnosis Department from the Neuropsychiatry Department. Patients were diagnosed with AD by clinical examination and using the Mini Mental State Examination (MMSE) and the Clinical Dementia Rating scale (CDR) as a measure of general cognitive performance.

Results: CA1 and subiculum subfields were significantly reduced in size in patients with Alzheimer's disease in relation to the age-matched control group ($P < 0.05$). This finding was positively correlated with the MMSE score and negatively correlated with CDR clinical tests. No significant atrophy was found among other hippocampal subfields in the patients' group.

Conclusion: This study proposed a new approach to detect atrophy in hippocampal subfields, using MR volumetric study of high-resolution T1 images, that can be used as a biomarker in the diagnosis of AD patients and differentiating them from elderly control subjects which is important in early diagnosis of AD and hence the proper treatment to improve the prognosis of the cognitive function.

Background

Alzheimer's disease (AD) is the most common cause of dementia in the elderly population. It is progressively deteriorating different cognitive and behavioral domains causing serious effects on the quality of life of patients and their family members, and eventually, AD contributes to death. The diagnosis of AD usually involves clinical assessments, cognitive tests, and brain imaging. Early and accurate diagnosis of AD can help to delay the decline of the cognitive functions of the patients for months or years and also help in early initiation of treatment [1].

AD is characterized pathologically by the presence of abundant extracellular amyloid neuritic plaques and intracellular neurofibrillary tangles (NFTs) [1–3], the hippocampus and entorhinal cortex were found to be the first sites of pathological changes [4], and these changes are present years or even decades before the onset of the clinical manifestations of the disease.

* Correspondence: Mohamed86_9@hotmail.cm
[2]Radiodiagnosis Department, Faculty of Medicine, Tanta University, Tanta, Egypt
Full list of author information is available at the end of the article

The most widely used clinical criteria for the diagnosis of AD are the National Institute of Neurological and Communicative Disorders and Stroke Alzheimer's Disease and Related Disorder Association (NINDS-ADRDA) criteria and Mini Mental Status Examination (MMSE). Developments in magnetic resonance imaging (MRI) have greatly improved the understanding of AD. MRI enables us to visualize structural, metabolic, and functional changes. Medial temporal lobe atrophy can be associated with the disease [5].

Unfortunately, this has been found to have limited utility both in early disease and in the differentiation of AD from other causes of dementia and from normal aging [6]. In other words, by conventional MRI means, atrophy of the hippocampus and entorhinal cortex can be assessed using simple validated scales [7]; however, there is an overlap with age-related atrophy cases that makes the distinction of AD from normal aging more problematic in the elderly to achieve an accurate and reliable assessment using a human rater [8].

Volumetric analyses of brain structures have become increasingly common for diagnostic purposes and for identifying disease progression. It has been demonstrated that atrophy of the medial temporal lobe (MTL) memory structures, where the pathological changes of AD in terms of neurofibrillary tangles and neuronal loss first occur [2], can be detected even in subjects with mild cognitive impairment (MCI) [9, 10].

Accurate regional segmentation on MR images is necessary to obtain the volumetric measurements for various structures as the conventional approach based on signal intensity alone is not sufficient to distinguish between different structures as observed and characterized by Fischl et al. [11].

The hippocampus has a critical role in declarative and episodic memory, as well as a focus of structural change in normal aging [12] and diseases such as epilepsy and Alzheimer's disease (AD) [13].

The hippocampal formation consists of a number of distinct, interacting subfields (Figs. 1 and 2). Despite its internal complexity, limited MRI resolution previously forced researchers to model the hippocampus as a single, homogeneous structure in neuroimaging studies of aging and AD [14].

Even though studies have shown that whole hippocampal volumes derived from segmented MRI scans are powerful biomarkers for AD [11, 15], treating the hippocampus as a single entity disregards potentially useful information about its subfields (Fig. 3); they are also thought to play different roles in memory and learning [16, 17] and to be affected differently by AD and normal aging—as indicated by ex vivo, histological studies [18].

Studies have shown that atlas-based volumetric analysis found that even hippocampal subfields have specific changes and neurodegenerative atrophy patterns associated with AD and can distinguish different diagnostic groups.

Methods

This study was conducted on a total of 45 subjects: 15 controls (9 men, 6 women) with mean age 62.4 years (± 6.2), ranging from 56 to 69 years old, and 30 Alzheimer's disease patients (17 men, 13 women) with mean age 64.5 years (± 3.3), ranging from 58 to 70 years old; this
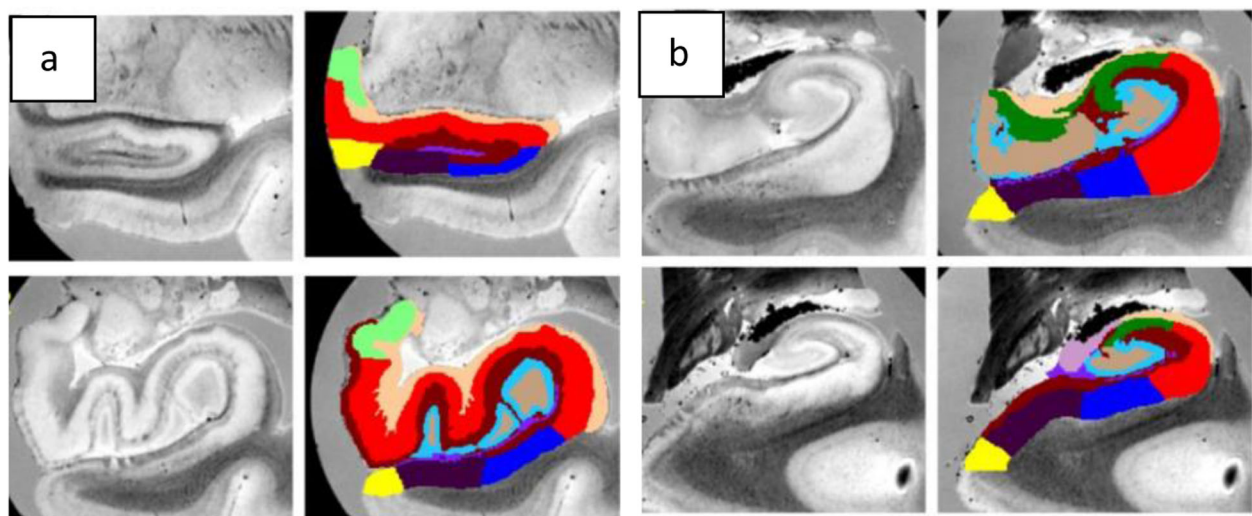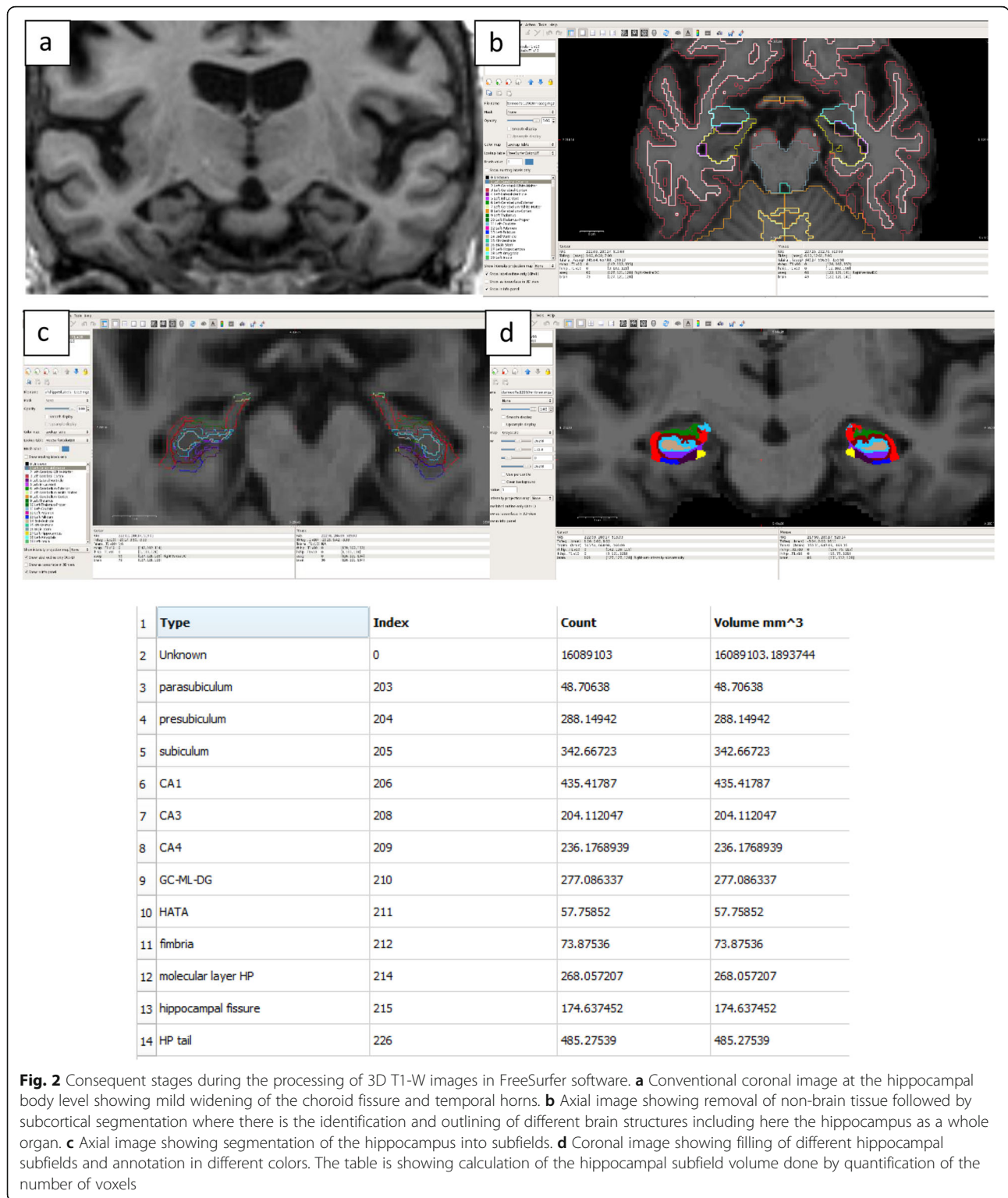

Fig. 1 Four coronal slices for hippocampal head and body with corresponding manual annotations. The slices are ordered from anterior to posterior. Red = CA1, blue = subiculum, dark purple = presubiculum, yellow = parasubiculum, cyan = granule cell layer of the dentate gyrus (GC-DG), light green = hippocampus-amygdala-transition-area (HATA)

1	Type	Index	Count	Volume mm^3
2	Unknown	0	16089103	16089103.1893744
3	parasubiculum	203	48.70638	48.70638
4	presubiculum	204	288.14942	288.14942
5	subiculum	205	342.66723	342.66723
6	CA1	206	435.41787	435.41787
7	CA3	208	204.112047	204.112047
8	CA4	209	236.1768939	236.1768939
9	GC-ML-DG	210	277.086337	277.086337
10	HATA	211	57.75852	57.75852
11	fimbria	212	73.87536	73.87536
12	molecular layer HP	214	268.057207	268.057207
13	hippocampal fissure	215	174.637452	174.637452
14	HP tail	226	485.27539	485.27539

Fig. 2 Consequent stages during the processing of 3D T1-W images in FreeSurfer software. **a** Conventional coronal image at the hippocampal body level showing mild widening of the choroid fissure and temporal horns. **b** Axial image showing removal of non-brain tissue followed by subcortical segmentation where there is the identification and outlining of different brain structures including here the hippocampus as a whole organ. **c** Axial image showing segmentation of the hippocampus into subfields. **d** Coronal image showing filling of different hippocampal subfields and annotation in different colors. The table is showing calculation of the hippocampal subfield volume done by quantification of the number of voxels

was done in the time period from 2016 to 2018. The patients were referred to the Radiodiagnosis Department and the controls were among their relatives and caregivers. Then approval of Research Ethics Committee (REC) of Tanta University and written consent were obtained from all studied participants. Inclusion criteria were patients who have been diagnosed with Alzheimer's disease by clinical examination, after fulfilling the National Institute of Neurological and Communicative Disorders and Stroke and the Alzheimer's Disease and
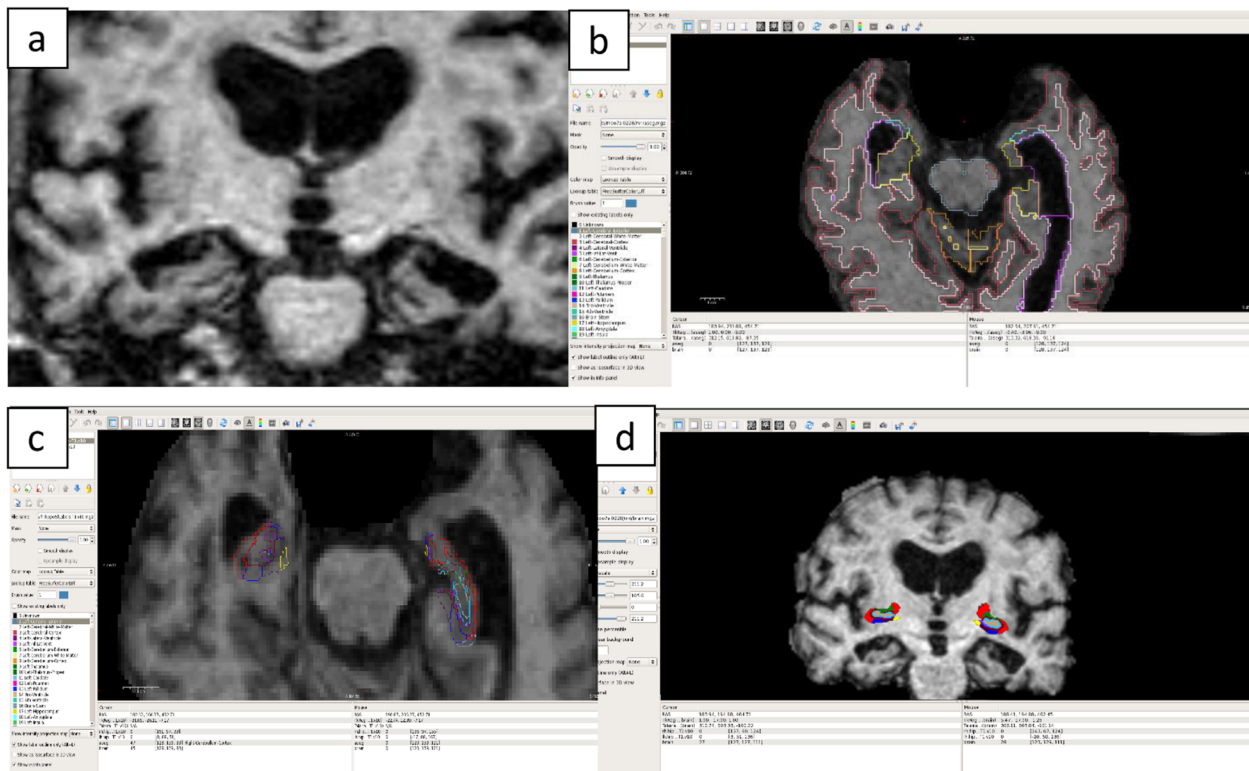
1	Type	Index	Count	Volume mm^3
2	Unknown	0	5896234	11055439.1893
3	parasubiculum	203	52.54107	52.54107
4	presubiculum	204	283.09453	283.09453
5	subiculum	205	334.0451	334.0451
6	CA1	206	430.25077	430.25077
7	CA3	208	206.37638	206.37638
8	CA4	209	235.07752	235.07752
9	GC-ML-DG	210	280.14802	280.14802
10	HATA	211	57.693581	57.693581
11	fimbria	212	69.91271	69.91271
12	molecular layer HP	214	264.02129	264.02129
13	hippocampal fissure	215	163.02509	163.02509
14	HP tail	226	479.7066	479.7066

Fig. 3 Consequent stages during the processing of 3D T1-W images in FreeSurfer software. **a** Conventional coronal image at the hippocampal body level showing moderate widening of the choroid fissure and temporal horns. **b** Axial image showing removal of non-brain tissue followed by subcortical segmentation where there is identification and outlining of different brain structures including here the hippocampus as a whole organ. **c** Axial image showing segmentation of the hippocampus into subfields. **d** Coronal image showing filling of different hippocampal subfields and annotation in different colors. The table is showing calculation of the hippocampal subfields volume done by quantification of the number of voxels

Related Disorders Association (NINCDS-ADRDA), Diagnostic and Statistical Manual of Mental Disorders IV (DSM IV) criteria, MMSE score ranged from 9 to 23, and CDR score from 1 to 3. All individuals of the study were subjected to full history taking, thorough clinical examination, and routine laboratory investigations in the form of CBC, liver and kidney function test, fasting and 2-h postprandial blood glucose, ESR, LDH, and CRP to exclude diseases that affect the conscious level and memory function. Exclusion criteria included dementia of other types other than Alzheimer's disease, systemic illness or organ failure, and patients unable to do MRI who have a cardiac pacemaker or metallic prosthesis.

Image acquisition and post-processing
The images were acquired by using 1.5 Tesla GE closed configuration whole-body scanner using a standard quadrature head coil. The patients were entered head first in supine position. All patients were subjected to the following conventional MRI protocols: sagittal 3D T1-weighted spoiled gradient (SPGR) utilizing the following parameters—a repetition time (TR) of 7.2 ms, an echo time (TE) of 120 ms, a slice thickness of 1.2 mm, and FOV = 256 × 256 mm. A high spatial resolution (isotropic) three-dimensional (3D) T1-weighted spoiled gradient echo (SPGR) of 1.2 mm slice thickness with no spacing was obtained in sagittal plane, with preparation time of 500 ms and an imaging duration of 5–7 min per acquisition; a repetition time 7.2 ms and minimum full echo time; a flip angle of 10° (to partly compensate inhomogeneity in the radiofrequency field); 160 slices, encoding frequency 16 kHz, a field of view of 30 cm, and an acquisition matrix size of 192 × 192 (FH AP RL; FH = foot-to-head; AP = anteriorto-posterior; RL = right-to-left); and frequency DIR S/I, NEX 1.0 with active automated shimming. Phased-array uniformity enhancement (PURE) was applied and surface coil intensity correction (SCIC) was off. This protocol resulted in high-resolution images with high gray-white matter contrast, used for measuring of specific gray matter (hippocampus) region of interest.

MRI data preprocessing
The preprocessed images are lodged into the automated brain segmentation software FreeSurfer, then algorithm initiation and calculation of hyperparameters for subcortical segmentation.

Data processing technique
A sequence of steps is then performed by the software as following: removal of the skull and any remaining background noise from T1 images to produce a skull-stripped corrected volume that is used in the segmentation algorithm; spatial normalization process is then done to the volume to correct the displacements, rotations, and scales and bring the person's volume into Talairach space which is a standard morphological space; identification of the boundary of the gray/white matter interface as well as the pial surface; segmentation of the different brain anatomical structures, where different measures can be made; and the segmentation of the subcortical white matter and deep gray matter volumetric structures, such as the hippocampus. These structures can then be filled in different label colors.

Measurement of the hippocampal subfield volume ROI analysis
Further segmentation of the hippocampus is done and different subfields can be extracted to be labeled differently, and calculation of volume is then measurable and generated for each of the segmented hippocampal subfields (Fig. 4). The conventional images are interpreted by two neuroradiologists and one neurologist who have a medical doctorate degree and are experienced in neuroimaging for more than 10 years duration, and then the final volume measurements are the results of an automated processing which has no human rater involved.
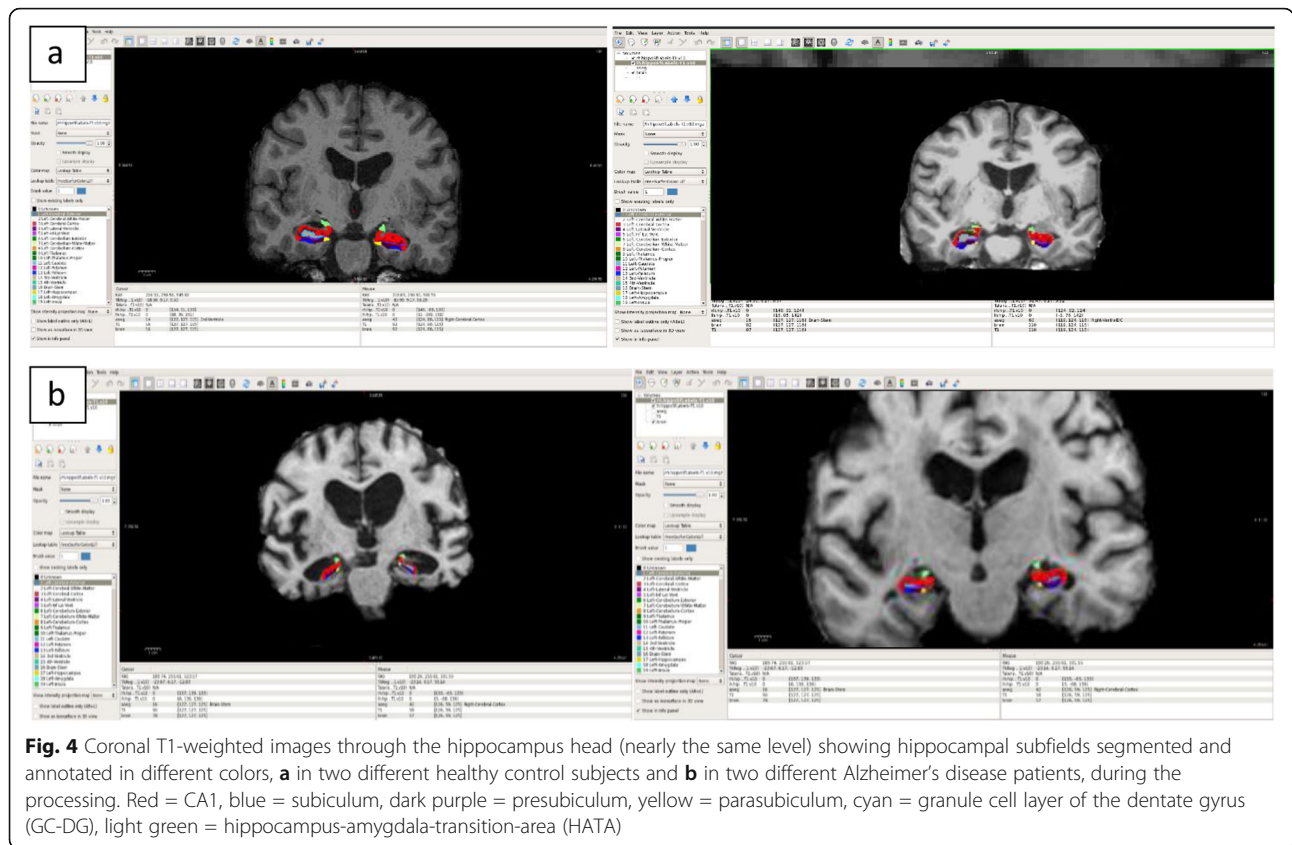
Statistical analysis of the data
Data were provided for the computer and analyzed using IBM SPSS software package version 20.0. To assess both the principal impacts of diagnosis (ADversus-control) factors on the hippocampal subfield volume, this work used analysis of covariance with total intracranial volume, education, sex, and age as nuisance variables.

Qualitative data were described using number and percent. Quantitative data were described using range, mean, standard deviation, and median. Comparison of MRI findings with normal values was done using one sample t test. Significant test results are quoted as two-tailed probabilities. The significance of the obtained results was judged at the 5% level. P value < 0.05 was considered significant.

Results
This study included 45 subjects: 15 controls (9 men, 6 women; mean age 62.4 ± 6.2 years) who were proved to be healthy and 30 Alzheimer's disease patients (17 men, 13 women; mean age 64.5 ± 3.3 years). The demographic data and cognitive scores for control and Alzheimer's disease cases are shown in Table 1. All patients were diagnosed by clinical examination, conventional MRI, and then hippocampal subfields volumetric measurements after segmentation with FreeSurfer (Fig. 4). The subiculum and CA1 subfield volumes in patients with Alzheimer's disease were significantly reduced on both sides in relation to age-matched controls (P < 0.05), and there was no significant difference found between both sides (Table 2).

Fig. 4 Coronal T1-weighted images through the hippocampus head (nearly the same level) showing hippocampal subfields segmented and annotated in different colors, **a** in two different healthy control subjects and **b** in two different Alzheimer's disease patients, during the processing. Red = CA1, blue = subiculum, dark purple = presubiculum, yellow = parasubiculum, cyan = granule cell layer of the dentate gyrus (GC-DG), light green = hippocampus-amygdala-transition-area (HATA)

They were found to have a positive correlation with the MMSE score which proved to be statistically significant when compared with normal elderly subjects; correlation coefficient (r) was 0.971, 0.957, 0.98, and 0.987 for right CA1, right subiculum, left CA1, and left subiculum, respectively (Table 3).

Meanwhile, they showed a negative correlation with the CDR score which was also statistically significant when compared with normal elderly subjects; correlation coefficient (r) was − 0.892, − 0.879, − 0.917, and − 0.871 for right CA1, right subiculum, left CA1, and left subiculum, respectively (Table 3).

Other studied subfields that were decreased could not be proved to be statistically significant. There was no significant correlation between group differences in age, sex, or years of education. Sensitivity, specificity, PPV and NPV of CA1, and subiculum volume reduction in AD relative to healthy elderly control were high, and the sensitivity of the study is increased by combination between volumes and the clinical exam scores.

Discussion

Alzheimer's disease is the most common cause of dementia in elderly people, and it is a progressive disease

Table 1 Demographic data and cognitive score

	HC ($n = 15$)	AD ($n = 30$)			P value
		Mild*	Moderate	Severe	
Gender (male/female)	9/6	7/4	8/9	2/0	0.09
Age	62.4 + 6.2	62.4 + 2.7	65.7 + 2.9	66 + 1	0.07
Years of education	14.1 + 3.6	12.2 + 1.7	11.2 + 1.4	12.5 + 0.5	0.027
MMSE score	27.67 + 1.74	21.5 + 1.4	14.4 + 2.5	9 + 0	0.02
Clinical dementia rating (CDR)**	–	1 + 0.3	2 + 0.1	3 + 0	0.6
Years from diagnosis	–	3.5 + 1.2	4.7 + 1.3	6.25 + 0.8	N/A

P value < 0.05 is significant
R correlation coefficient

Table 2 Subiculum and CA1 subfields mean volumetric measurements in patients and control groups

Subfields	Patients (mean in mm^3)	Control (mean in mm^3)	*P* value
Right subiculum	344.6655	488.7813	0.009404
Right CA1	506.885	693.6842	0.026623
Left subiculum	357.9499	476.5698	0.03426
Left CA1	497.4369	686.2935	0.021111

P value < 0.05 is significant

and its prevalence is predictable to increase as populations continue to age around the world. It is associated with neurofibrillary tangles and neuritic plaques, along with other changes as well as amyloid angiopathy and age-related brain atrophy which may contribute to cognitive impairment [19].

The hippocampus was found to have a special affinity for AD pathology and considered an early site for involvement, so hippocampal atrophy is used to be an imaging marker of AD and included in the diagnostic criteria [20].

Visual rating methods used in the assessment of the volume of the medial temporal lobe and the size of the surrounding CSF spaces showed obviously that they are lacking the accuracy in anatomical segmentation, as a result has low sensitivity and specificity for distinguishing AD from normal subjects with senile changes. In other words, there were dementia subjects with minimal MTA score who have only increased width of the choroid fissure without the temporal horn dilatation and were found to have already established regionally pronounced hippocampal atrophy by volumetric means. It was noted also that cases showing some degree of temporal horn dilatation in conventional imaging could have normal volumetric studies without any significant atrophy [21].

This study aimed to identify a specific regional atrophy pattern characteristic for Alzheimer's disease in comparison to normal age-matched control, and this could enable us to better understand the course of the disease and help in its early effective treatment. FreeSurfer software was used for automated hippocampal segmentation using the preprocessed images, after initiation of the segmentation algorithm and calculation of hyperparameters and then using the output to calculate their volumes. Volumes were normalized by the intracranial volume and the gray matter volume [22].

One of the advantages of FreeSurfer software is that it is applicable for images produced by any MRI machine. Patients were classified according to MMSE and CDR clinical examinations into mild, moderate, and severe groups. The mean age of each group was 62.4, 65.7, and 66 years for mild, moderate, and severe groups, respectively. The number of years of education was included in the criteria, and their means for the three groups were 12.2, 11.2, and 12.5 years, respectively. The patients also had mean number of years since first diagnosed as AD: 3.5, 4.7, and 6.25 years for the three groups, respectively. They had presented variable medial temporal lobe atrophy-MTA scores and white matter lesion FAZKEAS scale.

After the segmentation process of the hippocampal subfields, it was found that both subiculum and CA1 on both sides had significantly reduced volumes in AD patients relative to the control group. This finding is matching with other previous studies as Kerchner et al. [23] , Zhao et al. [24], and Trujillo-Estrada et al. [25] which suggested the involvement of CA1 and subiculum subfields in particular.

These findings were correlated with the MMSE and CDR scores. All results showed significant *P* value and correlation. Correlation to age was determined by Pearson's correlation coefficient. The other subfields showed no significant volume differences between AD and controls.

This work is also matching with recent studies; Hett et al. [26] have presented in their study that CA1 and subiculum are the subfields which show the most significant atrophy in AD. Also, Zhao et al. [24] has found that significant atrophy is seen in CA1, subiculum, presubiculum, molecular layer, and fimbria subfields among subjective mild cognitive decline, amnestic mild cognitive impairment, and Alzheimer's groups; they in turn

Table 3 Correlation between the volumes of CA1 and subiculum in mm^3 in AD patients and MMSE and CDR scores

Mean hippocampal subfield volumes	HC (*n* = 15)	AD (*n* = 30)			*P* value	*R* score (MMSE/CDR)
		Mild	Moderate	Severe		
Right CA1	693.68 + 40.25	602.05 + 29.7	462.21 + 41.04	410.26 + 4.39	< 0.00001	0.9711/− 0.8921
Right subiculum	488.78 + 38.95	390.59 + 14.46	330.81 + 23.89	250.63 + 35.33	< 0.00001	0.9579/− 0.8793
Left CA1	686.29 + 36.72	583.97 + 34.22	458.03 + 33.67	402.04 + 8.89	< 0.00001	0.9801/− 0.9174
Left subiculum	476.57 + 28.45	386.03 + 5.43	347.83 + 16.55	312.29 + 0.89	< 0.00001	0.9875/− 0.8715

P value < 0.05 is significant
R correlation coefficient

Saad *et al. Egyptian Journal of Radiology and Nuclear Medicine*   (2020) 51:53

Page 8 of 9

had suggested that this could be used as a biomarker in early stages of AD. Using the same image analysis approach, Hanseeuw et al. [27] showed some difference as their study reported significant volume losses in the subiculum and CA2-3 subfields in a small group of 15 amnestic MCI subjects and 15 healthy controls.

Mueller et al. [28] evaluated correlations between subfield volumes and two different memory scores based on the California Verbal Learning Test in a mixed group including cognitively normal healthy controls with a subjective memory complaint and patients with cognitive impairment, and it was found that atrophy of CA subfields appear to be related to associative memory dysfunction observed in patients with cognitive impairment. In a similar way, analysis was run on 490 individuals (including controls, MCI, and AD patients), and the authors did not find any specific correlates in healthy controls, while regions corresponding to CA1 and subiculum were associated with delayed recall performances in patients [29].

An automated hippocampal shape-analysis method by using a pattern-recognition algorithm revealed a positive correlation between CERAD delayed recall scores and hippocampal deformation in the CA1 and subiculum [30].

The earlier postmortem pathologic studies showed that degeneration of the CA1 and subiculum found to be more severe as compared with other hippocampal components in early stages of AD, and these findings are correlated with this study. Human autopsy studies suggest that volume loss of subiculum and CA1 is related to the number of neurofibrillary tangles in these areas, neuronal loss, loss of dendritic arbor, or afferent innervation. Previous studies suggested that marked degeneration of the perforant path, that is providing input from layer III of entorhinal cortex to CA1 and subiculum, was a characteristic feature of AD [29].

However, CA3 and the DG, in contrast to subiculum and CA1, are not affected by the formation of plaques, tangles, and neuronal loss until a later stage in AD [31]. Mueller et al. [28] found that atrophy of CA subfields, as grouped together in a single region, appear to be related to associative memory dysfunction observed in patients with cognitive impairment and correlate with incapability of the patients to benefit from semantic processing during encoding new information. In a similar way, analysis was run on 490 individuals (including controls, MCI, and AD patients from the Alzheimer's disease neuroimaging initiative), and the authors did not find any specific correlates in healthy controls, while regions corresponding to CA1 and subiculum were associated with delayed recall performances in patients. A reliable result appears to determine the role of CA1 atrophy in memory dysfunction in MCI and AD [29]. The results of this

study reveal that sensitivity, specificity, PPV and NPV of CA1, and subiculum volume reduction in AD in relation to healthy elderly control were high, and the sensitivity of the study is increased by combination between volumes and the clinical exam scores. Limitations of this study are firstly that it is not possible to separate the temporal relation between subfield volume changes and the clinical symptoms because of its design as a cross-sectional study, and secondly, the relatively small number of studied subjects. Future longitudinal study and larger sample size combined with other biomarkers will be needed to determine which hippocampal subfields show the earliest atrophy in the disease process and to confirm the findings.

Conclusion

This work has proposed a new approach to better capture Alzheimer's disease. Reduced CA1 and subiculum volumes is seen in patients with Alzheimer's disease. Further studies are needed to integrate these findings in the routine workup in evaluating patients with AD.

Consent for publication

All patients included in this research gave written informed consent to publish the data contained within this study. If the patient was unconscious when consent for publication was requested, written informed consent for the publication of this data was given by their legal guardian. I confirm that the content of the manuscript has not been published or submitted for publication elsewhere.

Competing interests

The authors declare that they have no competing interests.

Author details

[1]Tanta Menshawy Hospital, Tanta, Egypt. [2]Radiodiagnosis Department, Faculty of Medicine, Tanta University, Tanta, Egypt. [3]Neuropsychiatry Department, Faculty of Medicine, Tanta University, Tanta, Egypt.

References

1. DeTure MA, Dickson DW (2019) The neuropathological diagnosis of Alzheimer's disease. Mol Neurodegeneration 14(1):32
2. Braak H, Braak E (1991) Neuropathological stageing of Alzheimer-related changes. Acta Neuropathologica 82(4):239–259
3. Mirra SS, Heyman A, McKeel D, Sumi SM, Crain BJ, Brownlee LM et al (1991) The Consortium to Establish a Registry for Alzheimer's Disease (CERAD). Neurology 41(4):479
4. O'Brien JT, Metcalfe S, Swann A, Hobson J, Jobst K, Ballard C et al (2000) Medial temporal lobe width on CT scanning in Alzheimer disease: comparison with vascular dementia, depression and dementia with Lewy bodies. Dement Geriatr Cogn Disord 11(2):114–118
5. Jobst KA, Smith AD, Szatmari M, Molyneux A, Esiri ME, King E (1992) Detection in life of confirmed Alzheimer's disease using a simple measurement of medial temporal lobe atrophy by computed tomography. Lancet 340(8829):1179–1183
6. Dekeyzer S, De Kock I, Nikoubashman O, Vanden Bossche S, Van Eetvelde R, De Groote J et al (2017) "Unforgettable" - a pictorial essay on anatomy and pathology of the hippocampus. Insights Imaging 8(2):199–212
7. Goos JD, Kester MI, Barkhof F, Klein M, Blankenstein MA, Scheltens P et al (2009) Patients with Alzheimer disease with multiple microbleeds: relation with cerebrospinal fluid biomarkers and cognition. Stroke 40(11):3455–3460
8. de Leon MJ, DeSanti S, Zinkowski R, Mehta PD, Pratico D, Segal S et al (2004) MRI and CSF studies in the early diagnosis of Alzheimer's disease. J Intern Med 256(3):205–223
9. De Santi S, de Leon MJ, Rusinek H, Convit A, Tarshish CY, Roche A et al (2001) Hippocampal formation glucose metabolism and volume losses in MCI and AD. Neurobiol Aging 22(4):529–539
10. Du AT, Schuff N, Kramer JH, Rosen HJ, Gorno-Tempini ML, Rankin K et al (2007) Different regional patterns of cortical thinning in Alzheimer's disease and frontotemporal dementia. Brain 130(4):1159–1166
11. Fischl B, Salat D, Busa E, Albert M, Dieterich M, Haselgrove C et al (2002) Whole brain segmentation: automated labeling of neuroanatomical structures in the human brain. Neuron 33(3):341–355
12. Frisoni GB, Ganzola R, Canu E, Rüb U, Pizzini FB, Alessandrini F et al (2008) Mapping local hippocampal changes in Alzheimer's disease and normal ageing with MRI at 3 Tesla. Brain 131(12):3266–3276
13. Apostolova LG, Dinov ID, Dutton RA, Hayashi KM, Toga AW, Cummings JL et al (2006) 3D comparison of hippocampal atrophy in amnestic mild cognitive impairment and Alzheimer's disease. Brain 129(11):2867–2873
14. Boccardi M, Ganzola R, Bocchetta M, Pievani M, Redolfi A, Bartzokis G et al (2011) Survey of protocols for the manual segmentation of the hippocampus: preparatory steps towards a joint EADC-ADNI harmonized protocol. J Alzheimers Dis 26(3):61–75
15. den Heijer T, Geerlings MI, Hoebeek FE, Hofman A, Koudstaal PJ, Breteler MM (2006) Use of hippocampal and amygdalar volumes on magnetic resonance imaging to predict dementia in cognitively intact elderly people. Arch Gen Psychiatry 63(1):57–62
16. Kesner RP (2013) An analysis of the dentate gyrus function. Behav Brain Res 254:1–7
17. Reagh ZM, Watabe J, Ly M, Murray E, Yassa MA (2014) Dissociated signals in human dentate gyrus and CA3 predict different facets of recognition memory. J Neurosci 34(40):13301–13313
18. Braak E, Braak H (1997) Alzheimer's disease: transiently developing dendritic changes in pyramidal cells of sector CA1 of the Ammon's horn. Acta Neuropathol 93:323–325
19. Pradier C, Sakarovitch C, Le Duff F, Layese R, Metelkina A, Anthony S et al (2014) The mini mental state examination at the time of Alzheimer's disease and related disorders diagnosis, according to age, education, gender and place of residence: a cross-sectional study among the French National Alzheimer database. PloS One 9(8):e103630
20. Mufson EJ, Mahady L, Waters D, Counts SE, Perez SE, DeKosky ST et al (2015) Hippocampal plasticity during the progression of Alzheimer's disease. Neuroscience 309:51–67
21. Todd MT, Nystrom LE, Cohen JD (2013) Confounds in multivariate pattern analysis: theory and rule representation case study. Neuro Image 77:157–165
22. Iglesias JE, Augustinack JC, Nguyen K, Player CM, Player A, Wright M et al (2015) A computational atlas of the hippocampal formation using ex vivo, ultra-high resolution MRI: application to adaptive segmentation of in vivo MRI. Neuroimage 115:117–137
23. Kerchner GA, Deutsch GK, Zeineh M, Dougherty RF, Saranathan M, Rutt BK (2012) Hippocampal CA1 apical neuropil atrophy and memory performance in Alzheimer's disease. Neuroimage 63(1):194–202
24. Zhao W, Wang X, Yin C, He M, Li S, Han Y (2019) Trajectories of the hippocampal subfields atrophy in the Alzheimer's disease: a structural imaging study. Front Neuroinform 13:13
25. Trujillo-Estrada L, Dávila JC, Sánchez-Mejias E, SanchezVaro R, Gomez-Arboledasa A, Vizueteb M et al (2014) Early neuronal loss and axonal/presynaptic damage is associated with accelerated amyloid-β accumulation in aβpp/ps1 Alzheimer's disease mice subiculum. J Alzheimers Dis 42(2):521–541
26. Kilian Hett, Vinh-Thong Ta, José Manjón, Pierrick Coupé (2018) Graph of hippocampal subfields grading for Alzheimer's disease prediction. Machine Learning in Medical Imaging hal-01859257
27. Hanseeuw BJ, Van Leemput K, Kavec M, Grandin C, Seron X, Ivanoiu (2011) A Mild cognitive impairment: differential atrophy in the hippocampal subfields. AJNR Am J Neuroradiol 32(9):1658–1661
28. Mueller SG, Chao LL, Berman B, Weiner MW (2011) Evidence for functional specialization of hippocampal subfields detected by MR subfield volumetry on high resolution images at 4 T. Neuroimage 56(3):851–857
29. Apostolova LG, Thompson PM, Green AE, Hwang KS, Zoumalan C, Jack CR Jr et al (2010) 3D comparison of low, intermediate, and advanced hippocampal atrophy in MCI. Hum Brain Mapp 31(5):786–797
30. Costafreda SG, Dinov ID, Tu Z, Shi Y, Liu CY, Kloszewska I et al (2011) Automated hippocampal shape analysis predicts the onset of dementia in mild cognitive impairment. Neuroimage 56:212–219
31. Lindberg O, Walterfang M, Looi JC, Malykhin N, Ostberg P, Zandbelt B et al (2012) Hippocampal shape analysis in Alzheimer's disease and frontotemporal lobar degeneration subtypes. J Alzheimers Dis 30(2):355–365

Publisher's Note

Springer Nature remains neutral with regard to jurisdictional claims in published maps and institutional affiliations.